Integrative Theory/Experiment-Driven Exploration of a Multicomponent Reaction towards Imidazoline-2-(thi)ones

Kruithof, Art; Mulder, Jos R.; Ruiz, J. M.; Janssen, Elwin; Mooijman, M.; Ruijter, Eelco; Guerra, Celia Fonseca; Bickelhaupt, F. Matthias; Orru, Romano V. A.

published in
European Journal of Organic Chemistry
2018

DOI (link to publisher)
10.1002/ejoc.201700941

document version
Publisher's PDF, also known as Version of record

ChemPubSoc Europe

DOI: 10.1002/ejoc.201700941

EurJOC European Journal of Organic Chemistry

Full Paper

Integrative Theory/Experiment | *Very Important Paper* |

VIP

Integrative Theory/Experiment-Driven Exploration of a Multicomponent Reaction towards Imidazoline-2-(thi)ones

Art Kruithof,[a] Jos R. Mulder,[a,b] J. M. Ruiz,[b] Elwin Janssen,[a] M. Mooijman,[a] Eelco Ruijter,[a] Célia Fonseca Guerra,[b,c] F. Matthias Bickelhaupt*[b,d] and Romano V. A. Orru*[a]

Abstract: Predicting reactivity in multicomponent reactions (MCRs) is extremely difficult. These reactions proceed by multiple pathways and are inherently associated with a potentially large variation of reactants and functional groups. To date, theoretical chemistry has been used in hindsight to verify experimental observations. However, its use in the early stages of the development of a (multicomponent) reaction process can prevent laborious and time-consuming optimization studies by pinpointing the most relevant parameter(s) in the reactivity, thus focusing experimental efforts. Herein, we discuss a study that truly integrates theoretical and synthetic chemistry to unravel in full detail the complex and intricate reaction characteristics of the novel versatile MCR of α-acidic iso(thio)cyanates, amines and aldehydes to access densely functionalized imidazoline-2-(thi)ones.

Introduction

Computational chemistry has developed from a niche between physics and chemistry to an explanatory tool for any chemist. By exploring reaction channels on the multidimensional potential energy surface (PES), a computational chemist is able to elucidate the reaction path(s) of any given reaction. Especially in the past decade, computational chemistry tools have advanced exponentially and are now at a highly sophisticated level.[1] The maturity of such computational tools should encourage synthetic chemists to routinely seek collaborations or employ these tools themselves as an integral part of rational reaction development.

We feel that a pragmatic approach making use of iterative theory/experiment cycles is needed to facilitate computational chemists to better aid synthetic chemists (and vice versa). In this way, the computational chemist may indeed identify a problematic part in a reaction pathway, thus helping the synthetic chemist to reduce the number of experiments to further explore desired reactivity or avoid non-desired reactivity. The acquired experimental data in turn serve as input for additional detailed computational clarification of reaction pathways and reaction outcomes.

We herein describe an approach that combines an initial thorough computational analysis of the reaction mechanism of a novel multicomponent reaction (MCR) with experimental benchmarking of a combinatorial set of reaction inputs (Figure 1). This should, on the one hand, confirm (or reject) the hypothesis on overall reactivity, but also provide information on additional or alternative (rate-)limiting factors. Then, in the

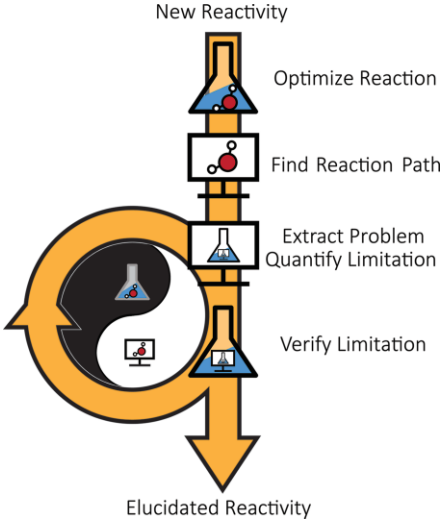

Figure 1. Our integrative methodology for iterative theory/experiment-driven multicomponent reaction exploration.

[a] *Department of Chemistry & Pharmaceutical Sciences and Amsterdam Institute for Molecules, Medicines & Systems (AIMMS), Vrije Universiteit Amsterdam, De Boelelaan 1108, 1081 HZ Amsterdam, The Netherlands E-mail: r.v.a.orru@vu.nl http://www.syborch.com*

[b] *Department of Theoretical Chemistry and Amsterdam Center for Multiscale Modeling (ACMM), Vrije Universiteit Amsterdam, De Boelelaan 1083, 1081 HV Amsterdam, The Netherlands E-mail: f.m.bickelhaupt@vu.nl http://www.chem.vu.nl/~bickel/*

[c] *Leiden Institute of Chemistry, Gorlaeus Laboratories, Leiden University, P. O. Box 9502, 2300 RA Leiden, The Netherlands*

[d] *Institute for Molecules and Materials (IMM), Radboud University, Heyendaalseweg 135, 6525 AJ Nijmegen, The Netherlands*

Supporting information and ORCID(s) from the author(s) for this article are available on the WWW under https://doi.org/10.1002/ejoc.201700941.

envisioned iterative process, the computational model system is improved to the next level of accuracy, guiding follow-up laboratory exploration of reaction scope.

MCRs offer a versatile platform for the combinatorial exploration of chemical space. Consequently, MCRs have developed into popular synthetic tools for medicinal chemists to efficiently access libraries of low-molecular-weight, drug-like compounds.[2]

The computational mechanistic analysis of the model system should disclose all intermediate steps of the reaction. Then, together with preliminary experimental results, a sound hypothesis for the (rate-)limiting step is developed. Subsequently, parametrization is used to account for any substituent effects, thereby creating a complete overall picture of the reaction characteristics. Although computational parametrization is a vibrant field with an increasing amount of predicting power,[3] the studies reported herein are focused on pragmatic methodology, which could be efficiently tailored to a particular reaction of choice.

To demonstrate our integrative theory/experiment-driven approach to reaction development, we focus here on a new MCR towards imidazoline-2-(thi)ones. These heterocycles represent important synthetic targets. For example, they have been recognized as kinase inhibitors,[4] protease inhibitors[5] and are used as precursors for N-heterocyclic carbenes.[6] Relevant to this work is our previously reported three-component reaction (3-CR) to access 2-imidazolines, a widely applied condensation of aldehydes/ketones, primary amines and isocyanides bearing an electron-withdrawing group at the α-position.[7] By employing empirical design principles based on literature and experimental data, we envisioned a single-reactant replacement (SRR) to arrive at a novel MCR to access imidazoline-2-(thi)ones of type **1** (Figure 2).

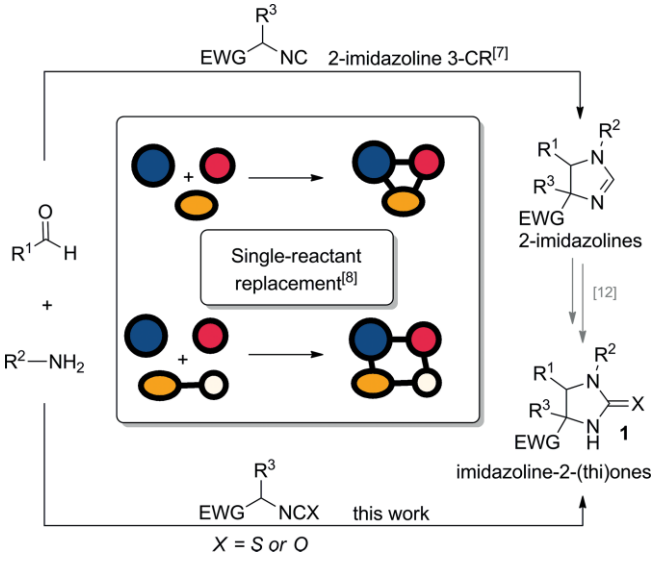

Figure 2. Design of a new MCR to access imidazoline-2-(thi)ones.

This SRR strategy involves systematic assessment of the mechanistic or functional role of each component in a known MCR and then replacement of one reactant with a different reactant displaying a similar reactivity mode required for the multicomponent condensation.[8] Considering that only the electron-withdrawing and electrophilic properties of the isocyanide functional group are exploited in the 3-CR towards 2-imidazolines, it may well be replaced by an iso(thio)cyanate to access imidazolidine-2-(thi)ones **1** instead.

Several (asymmetric) synthetic methods employing α-acidic isothiocyanates[9] for the synthesis of imidazoline-2-thiones have been reported; however, none employ the in situ formation of imines, thus leaving the advantages associated with MCRs unutilized. Furthermore, the known reports describe the employment of either harsh activation[10] or activated imines,[11] which narrow the potential scope of this reaction.

Finally, a one-step approach starting from readily available inputs (Figure 2) would be a significant improvement compared with our earlier multistep procedures to access imidazoline-2-(thi)ones **1**.[12]

Results and Discussion

Initially, we used readily available *p*-chlorobenzaldehyde (**2a**), *n*-butylamine (**3a**), and the iso(thio)cyanates **4** derived from *p*-chlorophenylglycine. Conveniently, compounds **4** can be prepared in one step starting from the corresponding amines by using (thio)phosgene and sodium carbonate.[13,14] The one-pot 3-CR of **2**, **3** and **4a** indeed gave the expected imidazoline-2-thione **1a**, which could be isolated in an excellent 93 % yield (Scheme 1). The pre-formation of the imine **5a** proved necessary to prevent side-product formation (**6a** and **7a**), and the addition of an external base, that is, pyridine, turned out to be unnecessary.[15] However, under these reaction conditions isocyanate **4b** failed to react with the pre-formed imine, and formation of the desired **1b** was not observed.

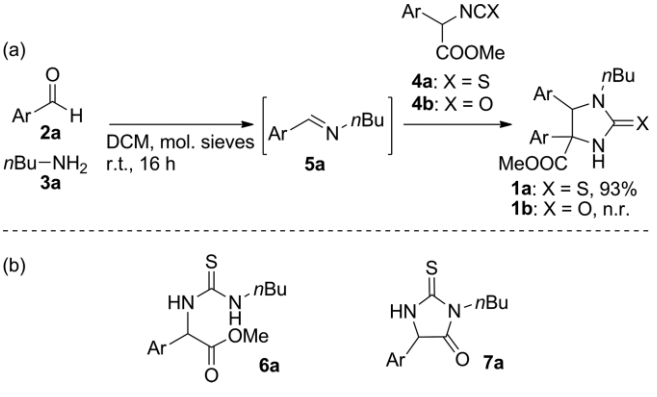

Scheme 1. Optimized reaction conditions and observed side-products. Ar = *p*-chlorophenyl.

The formation of **6a** and **7a** in the non-optimized reaction indicates that the 3-CR proceeds in a stepwise fashion, starting with the formation of the imine **5a** followed by (cyclo)addition of the isothiocyanate **4a**. The addition of an external base had no influence on the outcome of the reaction. Further, the (rate-)limiting step of this reaction lies before any irreversible

step at an early stage of the reaction pathway, as the use of isocyanate **4b** (X = O) did not result in product formation and only starting material was recovered.

After imine formation, the formal cycloaddition to give the imidazoline-2-(thi)one scaffold involves both carbon–carbon (C–C) and nitrogen–carbon (N–C) bond formation. Three pathways are conceivable: (1) first C–C and then N–C bond formation, (2) first N–C and then C–C bond formation and (3) simultaneous C–C and N–C bond formation.

In this respect, some of our earlier mechanistic findings on the cyclization reactions of imines **5** by using either α-acidic isocyanides **8** or nitrilium triflates **9** are relevant (Scheme 2). In the 3-CR towards 2-imidazolines, that is, the reaction of an imine with an α-acidic isocyanide, C–C bond formation precedes C–N bond formation.[7b,16] The deprotonated α-carbon atom of the isocyanide was postulated as the initial nucleophile. Later, we demonstrated that the reactions of imines and nitrilium triflates to access 2-arylimidazolines occur with an opposite order of events. DFT calculations showed here that the imine is more likely to attack the nitrilium ion.[17]

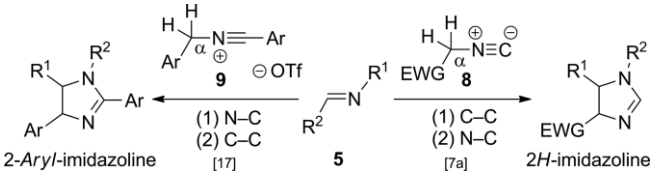

Scheme 2. Initial considerations from analogous imidazoline formations.

Taking the above into account, the addition/cyclization reaction of *N*-methylethanimine (**5b**) and methyl 2-isothiocyanato-2-phenylacetate (**4e**) was chosen as the model reaction for the initial DFT calculations in our current study. The fairly simple starting imine **5b** was chosen to reduce the number of atoms and degrees of freedom, therefore limiting the required computational resources. Additionally, this model system reduced the number of possible conformers, and thus conformer space could be covered efficiently (see the Supporting Information for all geometries). All the calculations were performed by using the Amsterdam Density Functional package[18] with the OLYP functional and a TZ2P basis set. Transition-state optimizations were performed by using QUILD,[19] solvent effects were taken into account by using the COSMO (DCM) model[20] and relativistic effects were taken into account explicitly by using the ZORA approach (see Computational Details).

Compared with the isocyanides in the related MCRs towards 2-imidazolines, iso(thio)cyanates **4** are more electrophilic. The nucleophilic attack of the imine nitrogen atom of **5b** on the isothiocyanate carbon atom in **4e** could be a possible first step; however, this event leading to **P** needs 21.8 kcal/mol to proceed (Scheme 3). Furthermore, the follow-up step in this path is a 1,2-unimolecular proton shift[21] leading to the endothermic formation of intermediate **Q** (27.3 kcal/mol), which disqualifies this as a likely pathway for our reaction.

Next, we turned to a C–C bond formation as the initial step in which the α-carbon atom of the isothiocyanate acts as a nucleophile. This can only occur after an initial α-deprotonation. For this, no external base proved necessary, apparently

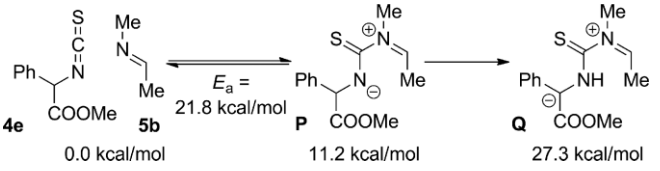

Scheme 3. Disqualification of N–C bond formation as the initial reaction step.

the in situ formed imine (Figure 3, green line) is sufficiently basic, resulting in ion pair **A1** (X = S). This initial proton transfer proves to be rate-limiting (17.4 kcal/mol). Activation of the imine to the iminium ion results in a relatively small barrier for the subsequent C–C bond formation. The nucleophilic attack of the α-carbanion on the iminium ion then gives the linear rotamers $\mathbf{B1}_{\alpha}$ and $\mathbf{B1}_{\beta}$ as the next intermediates in the pathway. Next, the rotamers $\mathbf{B1}_{\alpha+\beta}$ have to undergo C–C bond rotation providing $\mathbf{B1}_{\gamma-\zeta}$. After that, ring closure results in zwitterionic species **C1**. Deprotonation of *cis* isomers $\mathbf{C1}_{\alpha+\beta}$ by a second imine molecule leads in a concerted fashion to product ***1a-cis***. However, in the case of the *trans* isomer, a distinct ion pair **D1** is formed, which undergoes (partial) ion separation (**TS6**) followed by recombination to furnish product ***1a-trans*** (Figure 3).

Finally, the fact that the imine is needed to deprotonate the isothiocyanate disqualifies simultaneous C–C and N–C bond formations, as this is only possible with a neutral imine and a deprotonated α-carbon atom.[22]

With the complete reaction pathway for the model reaction charted (Figure 3, green line; for a complete overview see also the Supporting Information), we then turned to investigate the combination of isocyanate **4b** and **5b** (Figure 3, red line). Again, deprotonation of the α-carbon atom by the imine is the rate-determining step (20.6 kcal/mol). From the intermediate complex **A2**, the computations show that nucleophilic attack by the α-carbanion of **4b** on the iminium carbon yields either the rotamers $\mathbf{B2}_{\alpha+\beta}$ or proceeds directly towards zwitterionic **C2** through a concerted ring closure. Although the transition vectors of the involved transition states **TS2** do not suggest immediate ring closure, the asynchronous ring closure proceeds in a consecutive fashion, as became evident from the attempted geometry optimization of $\mathbf{B2}_{\gamma-\zeta}$, which only results in **C2**. Finally, according to the computational model, the imine-facilitated proton shift results in products **1b**. Unlike the model pathway towards imidazoline-2-thiones **1a**, both ***1b-cis*** and ***1b-trans*** can only be formed via separate ion pairs (**TS6**).

The computations revealed the full reaction profiles using isothiocyanate **4a** or isocyanate **4b**. The initial ion-pair formation (**A**) seems the limiting factor for this reaction and forms the kinetic barrier. In the model system using isocyanate **4b**, this prevents the reaction from proceeding as here the kinetic barrier is significantly higher in energy compared with the case for **4a**. In other words, if the first barrier is overcome, C–C bond formation should occur and the reaction proceeds to form **1a** or **1b**.

Clearly, the height of the first barrier also depends on the nature of the imine employed and thus on the substituent groups R^1 and R^2 on the amine and aldehyde used. The initial

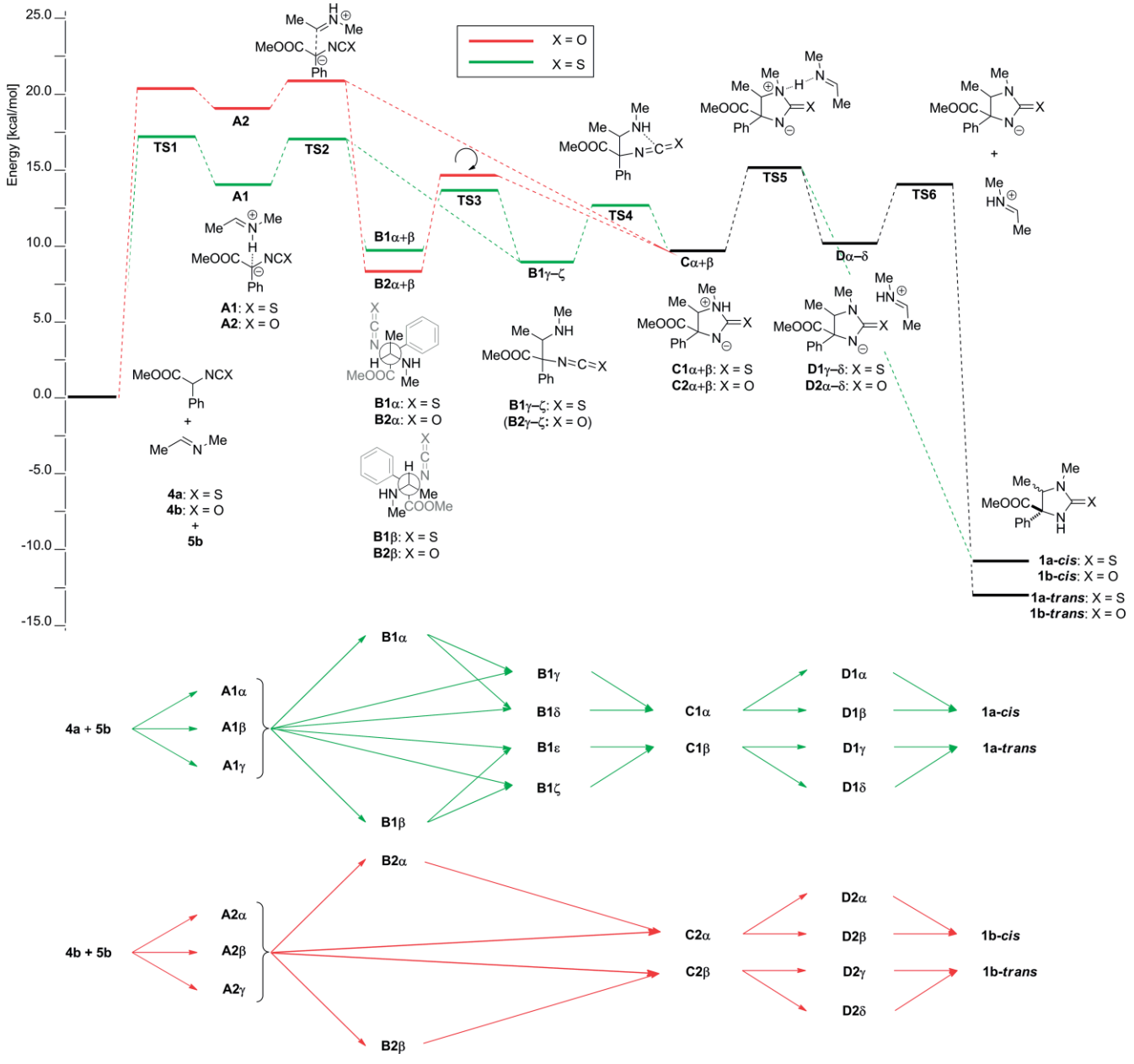

Figure 3. Reaction profile for the reaction between *N*-methylethanimine (**5b**) and phenylglycine-derived iso(thio)cyanates **4** (top) and specific routes for the various conformers and diastereoisomers (bottom).

kinetic barrier is determined mainly by the acidity of the α-proton in the iso(thio)cyanate and the basicity of the imine. The proton affinity (*PA*), which is defined as the change in enthalpy of removing a proton from its conjugated acid, has been used to computationally establish the acidity of a given system.[23] As such, the difference in proton affinity (Δ*PA*) between the two reaction partners used in our model may well serve to quantify the ability to form these acid/base ion pairs.

By using this approach only the Δ*PA* between either the isothiocyanate or the isocyanate on one hand and the imine on the other needs to be determined, thus avoiding the computationally much more expensive transition state and bimolecular geometry optimizations. In such an approach, indeed the relative thermodynamic stability of the separate ions will not exactly correspond to the kinetic barrier of the proton transfer. Consequently, the steric effects of the substituents, which could be of importance for the kinetics of the initial proton transfer and also for the stabilization of the resulting ion pair, were not taken into account. However, by using substituents of similar steric bulk, the effect becomes comparable for all computed ion pairs and we can in these cases neglect steric considerations. For the combination of imine **5a** with iso(thio)cyanates **4a** and **4b**, we performed these calculations and compared the results with the experimental outcome. The results depicted in Table 1 show that indeed the Δ*PA* seems to be a reliable parameter to predict product formation.

Table 1. ΔPAs [kcal/mol] of the inputs for the optimization study and of 9*H*-fluorenyl-substituted iso(thio)cyanates, namely **5a** with **4a**–**d**.

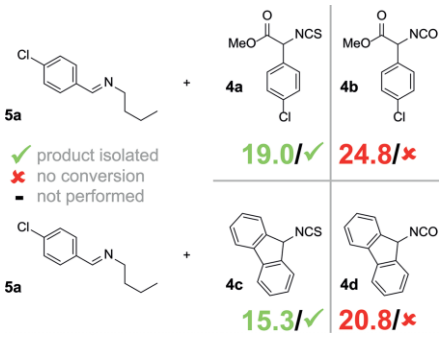

Next, we extended the test set of iso(thio)cyanates to **4c** and **4d** bearing the highly electron-withdrawing 9*H*-fluorenyl group. This functional group was also employed in our earlier studies on 3-CRs towards 2-imidazolines.[7a] Experimentally, only the use of isothiocyanate **4c** led to product formation, whereas isocyanate **4d** showed no conversion. After calculating the Δ*PA* values, this reactivity can again be explained by the (in)ability to form the initial ion pair (Table 1).

To map the influence of the imine, we picked nine different imines (**5c**–**5k**) derived from three representative amines and aldehydes (Table 2). In addition to **4c** and **4d**, we employed **4e** and **4f**, which are the phenyl analogues of **4a** and **4b**, respectively. Subsequently, the actual reactions for a selected sub-set of possible combinations were performed in the laboratory.[24] Conveniently, it proved unnecessary to perform all 36 possible reactions, because the computational results had already allowed us to establish the reactivity profile and identify borderline cases for expected reactivity. This additionally demonstrates the explanatory power of our approach. From Table 2, two observations stand out. First, input combinations **4e**–**5e** and **4e**–**5g** with a Δ*PA* of over 20 kcal/mol show product formation. Secondly, input combinations **4d**–**5c** and **4c**–**5f** (and **4c**–**5h**), with a significantly lower Δ*PA*, do not show any conversion. Additionally, the reactions that show some conversion indeed gave (partly) the expected imidazoline-2-thione product, which

Table 2. Computed Δ*PA* values [kcal/mol, green < 20 < red) and experimentally determined reactivity.[25]

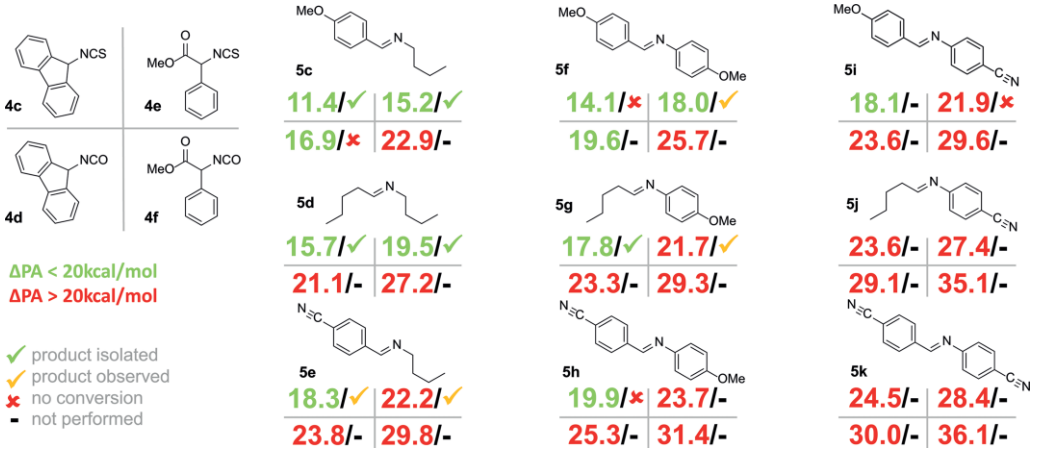

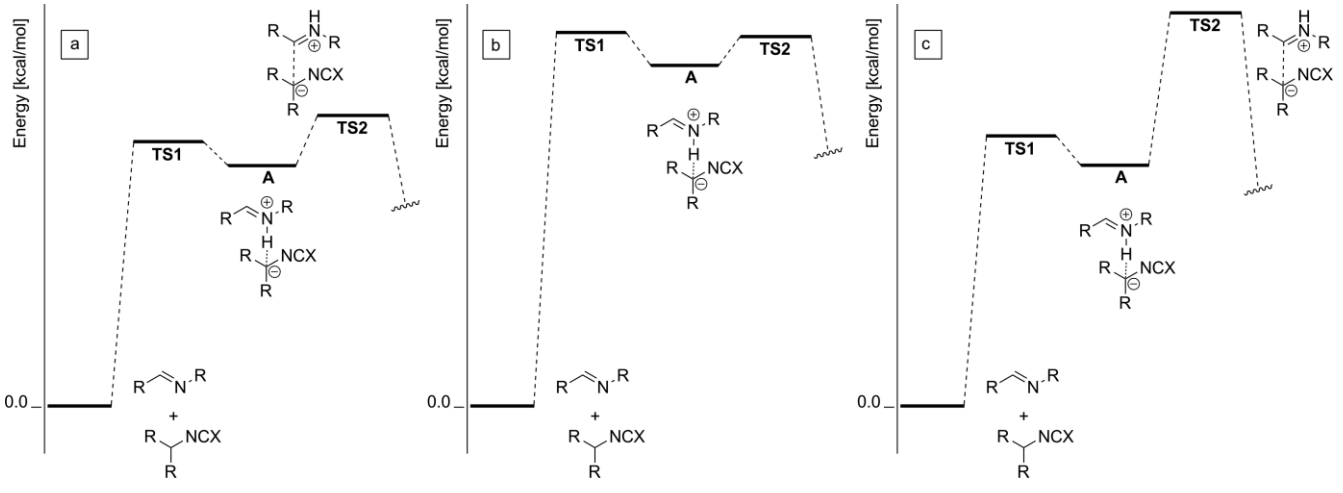

Figure 4. Extended hypothesis.

indicates that no additional significant barriers are encountered along the reaction coordinates. Consequently, in the reaction profile established above (Figure 3), this means that in addition to the ΔPA, the initial C–C bond formation must in some cases be involved as a rate-limiting step. Both experimental observations and our model system indicate that after this irreversible C–C bond formation, the reaction proceeds to the product without additional high kinetic barriers.

These observations led to a refined hypothesis accounting for the progress of our new 3-CR: in addition to the initial ion-pair formation, the C–C bond formation must also be involved as a possible rate-limiting step. As depicted in Figure 4a, when the reaction leads to the desired imidazoline-2-thione products, ion-pair formation is viable, and the carbon–carbon bond formation is sufficiently favoured for the reaction to proceed. In the case of a high ΔPA (Figure 4b), the reaction does not proceed, irrespective of the height of the second barrier. In the third scenario (Figure 4c), ion-pair formation is viable; however, the second barrier is too high in comparison with the proton transfer, and the reaction does not proceed.

Conclusions

We have reported an efficient and pragmatic methodology that integrates computational and experimental organic chemistry tools in an iterative fashion to drive multicomponent reaction exploration. We could efficiently study and predict the reaction mechanism as well as chart the scope and limitations of a new MCR towards imidazoline-2-(thi)ones. We observed a lack of reactivity for isocyanates in this reaction. Clarification of the reaction profile of a model system led to the extraction of a limiting parameter, that is, the difference in proton affinity (ΔPA) between the imine and the iso(thio)cyanate. This parameter was then used to computationally determine the scope and limitations and thus the performance of the reaction for a larger combinatorial set of possible inputs. Differences between the theoretical and experimental trends led to refinement of the reaction profile (C–C bond formation as a second decisive parameter). In general, we believe that using this integrative iterative theory/experiment methodology for reaction development leads to the fast elucidation of relevant reaction pathways, and a more effective charting of the scope and limitations of a novel reaction.

Experimental Section

Computational Details: All calculations were performed with the Amsterdam Density Functional (ADF) program developed by Baerends et al.[18] For transition-state optimizations the Quantum-regions Interconnected by Local Descriptions (QUILD) program was used.[19,26] The QUILD program is a wrapper around ADF (and other programs), which is used for its superior geometry optimizer, which is based on adapted delocalized coordinates. Molecular orbitals (MOs) were expanded by using the TZ2P basis set, which is an uncontracted set of Slater-type orbitals (STOs).[27] The TZ2P basis set is of triple-ζ quality, augmented by two sets of polarization functions (d and f on heavy atoms; 2p and 3d sets on hydrogen). Core electrons (e.g., 1s for second period, 1s2s2p for third period, 1s2s2p3s3p for fourth period, 1s2s2p3s3p3d4s4p for fifth period and 1s2s2p3s3p3d4s4p4d for sixth period) were treated by using the frozen core approximation.[18c] An auxiliary set of s, p, d, f, and g STOs was used to fit the molecular density and to represent the coulomb and exchange potentials accurately in each self-consistent field (SCF) cycle. Scalar relativistic corrections were included self-consistently by using the zeroth-order regular approximation (ZORA).[28] By using the OLYP density functional, energies, geometries and vibrational frequencies were calculated by using the local density approximation (LDA; Slater exchange[29] and VWN correlation[30]) with the gradient corrections of Handy–Cohen (exchange)[31] and Lee–Yang–Parr (correlation)[32] added self-consistently. The OLYP density functional is known as the best functional for the accuracy of geometries and the second best GGA functional for the energy barrier for S_N2 reactions.[23b] Solvent effects were taken into account in all calculations by using the COSMO model,[20] used explicitly both for solving the SCF equations and for geometry optimization. The solvent radius (R_s) for DCM was determined from experimental data for the macroscopic density (r) and molecular mass (M) with the formula $R_s^3 = 2.6752 \cdot M_m/\varrho$ leading to an R_s value of 2.94 Å for DCM; a value of 78.4 was used for the dielectric constant of water, and 8.9 was used for the dielectric constant of DCM. Atomic radii were taken from the MM3 van der Waals radii,[33] which are available for almost the whole periodic system, and scaled by 0.8333 (the MM3 radii are 20 % larger than the normal van der Waals radii due to the specific form of the van der Waals energy within the MM3 force field). The surface charges at the GEPOL93 solvent-excluding surface were corrected for outlying charges.[34] This setup provides a "non-empirical" approach to including solvent effects with a dielectric continuum, and works well for solvation processes.[7a] The non-electrostatic term in the ADF 2009 implementation of COSMO was set to zero, because this term is unphysical and also leads to unphysical binding at large distances. In the present version of the ADF program, this term has been removed. Geometries were optimized by using analytical gradient techniques until the maximum gradient component was less than 1.0×10^{-4} atomic units. All structures were verified by vibrational analyses to be minima structures (zero imaginary frequencies) or transition states (one imaginary frequency). Vibrational frequencies were obtained through numerical differentiation of the analytical gradients,[30] for which the GEPOL93 surface was recreated for all of the systems at each displaced geometry. For most systems, these standard settings resulted in too many imaginary frequencies (in the range of 0 to –200 cm^{-1}), which, however, proved to have positive values (of around 0–200 cm^{-1}) in the more accurate (automatic) *scanfreq* performed afterwards. The force constants of the imaginary frequencies were recalculated in *scanfreq* by numerical differentiation of the gradient at six points along the respective frequencies normal mode. The character of the normal mode associated with the imaginary frequency of a transition state (i.e., the transition vector) was analysed to ensure that the correct transition state was found. Vibrational energy effects (in particular, zero-point vibrational energy) and entropy effects were not considered in the calculations, because they have only a small influence on the energies obtained. Coordinates of all geometries can be found in the Supporting Information. Additionally, the Supporting Information contains a comprehensive illustration containing the structures of all investigated routes.

Experimental Details: All reactions were carried out under atmospheric conditions, unless stated otherwise. ^1H and ^{13}C NMR spectra were recorded with a Bruker Avance 250 (250.13 MHz for ^1H and 62.90 MHz for ^{13}C), Bruker Avance 400 (400.13 MHz for ^1H and 100.62 MHz for ^{13}C) or Bruker Avance 500 (500.23 MHz for ^1H and

125.70 MHz for ^{13}C) spectrometer with chemical shifts (δ) reported in ppm and internally referenced to residual solvent resonances of $CDCl_3$ (^1H: δ = 7.26 ppm; $^{13}C\{^1H\}$: δ = 77.0 ppm). Coupling constants (*J*) are reported in Hz, and all diastereoisomeric ratios (*dr*) were determined from crude spectra. IR spectra were obtained from neat samples utilizing a Shimadzu FTIR-8400s spectrophotometer. Electrospray ionization (ESI) MS was carried out with a micrOTOF-Q spectrometer in positive ion mode unless stated otherwise. Chromatographic purification refers to flash chromatography using the indicated solvent (mixture) and Baker 7024-02 silica gel (40 µ, 60 Å). TLC was performed by using silica plates from Merck (Kieselgel 60 F254 on aluminium with fluorescence indicator), and compounds were visualized by UV detection and I_2 staining unless stated otherwise. DCM was dried and freshly distilled from CaH_2 prior to use. All other commercial reagents, namely amines, aldehydes, pyridine, sodium carbonate and 9-isocyanato-9*H*-fluorene, were used without further purification. All iso(thio)cyanates failed to ionize on ESI-HRMS, both in positive and negative mode, and were therefore only analysed by ^1H and ^{13}C NMR and IR spectroscopy.

General Procedure 1: Either a solution of phosgene (1.0 M in toluene) or neat thiophosgene (1.3 equiv.) was added to a stirred solution of organic ammonium chloride (1.0 equiv.) and Na_2CO_3 (4 equiv.) in freshly distilled DCM at 0 °C. The resulting reaction mixture was warmed to room temperature and subsequently stirred for 7 d, filtered through Celite and concentrated in vacuo.

Methyl 2-(4-Chlorophenyl)-2-isothiocyanatoacetate (4a): According to general procedure 1, the reaction between 4-chlorophenylglycine methyl ester hydrochloride (12.6 g; 53.2 mmol), $CSCl_2$ (5.32 mL; 69.2 mmol) and Na_2CO_3 (22.6 g; 213 mmol) afforded **4a** as a yellow-brown oil (12.8 g, 100 %). ^1H NMR (250 MHz, $CDCl_3$): δ = 7.35 (s, 4 H), 5.06 (s, 1 H), 3.78 (s, 3 H) ppm. ^{13}C NMR (63 MHz, $CDCl_3$): δ = 170.1 (C), 135.0 (C), 133.8 (C), 132.3 (C), 129.2 (CH), 128.1 (CH), 62.0 (CH), 53.5 (CH_3) ppm (NCS carbon signal was not observed). IR (neat): $\tilde{\nu}_{max}$ = 2948, 2048, 2044, 1999, 1756, 1490, 1434, 1337, 1307, 1285, 1247, 1015 cm^{-1}.

Methyl 2-(4-Chlorophenyl)-2-isocyanatoacetate (4b): According to general procedure 1, the reaction between 4-chlorophenylglycine methyl ester hydrochloride (2.36 g, 10.0 mmol), $COCl_2$ (1.29 mL, 13.0 mmol) and Na_2CO_3 (5.68 g, 40.0 mmol) afforded **4b** as a yellow-brown oil (1.19 g, 100 %). ^1H NMR (250 MHz, $CDCl_3$): δ = 7.39–7.31 (m, 4 H), 5.06 (s, 1 H), 3.73 (s, 3 H) ppm. ^{13}C NMR (63 MHz, $CDCl_3$): δ = 167.6 (C), 135.5 (C), 132.4 (C), 129.3 (CH), 128.2 (CH), 62.2 (CH), 53.7 (CH_3) ppm (NCO carbon signal was not observed).

9-Isothiocyanato-9*H*-fluorene (4c): According to general procedure 1, the reaction between 9*H*-fluoren-9-amonium chloride (2.177 g, 10.0 mmol), $CSCl_2$ (1.0 mL, 13.0 mmol) and Na_2CO_3 (5.68 g, 40.0 mmol) afforded **4c** as a yellow-brown oil (2.23 g, 100 %). ^1H NMR (250 MHz, $CDCl_3$): δ = 7.71 (d, *J* = 7.5 Hz, 2 H), 7.66 (d, *J* = 7.5 Hz, 2 H), 7.46 (t, *J* = 7.5 Hz, 2 H), 7.38 (t, *J* = 7.5 Hz, 2 H), 5.73 (s, 1 H) ppm. ^{13}C NMR (63 MHz, $CDCl_3$): δ = 140.9 (C), 140.1 (C) 129.7 (2 CH), 128.2 (2 CH), 124.9 (2 CH), 120.4 (2 CH), 59.9 (CH) ppm. IR (neat): $\tilde{\nu}_{max}$ = 3065, 3043, 3020, 2179, 2152, 2083, 1607, 1475, 1450, 1288, 1180, 1150, 1105, 1072, 1018, 943, 874, 841, 789, 733 cm^{-1}.

Methyl 2-Isothiocyanato-2-phenylacetate (4e): According to general procedure 1, the reaction between (+)-(*S*)-2-phenylglycine methyl ester (2.14 g, 10.6 mmol), $CSCl_2$ (1.06 mL, 13.8 mmol) and Na_2CO_3 (4.49 g, 42.4 mmol) afforded **4e** as a dark-red oil (2.18 g, 100 %). ^1H NMR (500 MHz, $CDCl_3$): δ = 7.43–7.40 (m, 5 H), 5.29 (s, 1 H), 3.78 (s, 3 H) ppm. ^{13}C NMR (100 MHz, $CDCl_3$): δ = 168.0 (C), 139.9 (C), 134.0 (C), 129.5 (CH), 129.3 (2 CH), 126.9 (2 CH) 62.9, (CH), 53.7 (CH_3) ppm. IR (neat): $\tilde{\nu}_{max}$ = 2023, 1747, 1454, 1435, 1246, 1207, 1169, 984, 721, 692 cm^{-1}.

General Procedure 2: The amine (2.0 equiv.) and aldehyde (2.2 equiv.) were added to a flame-dried Schlenk flask charged with crushed molecular sieves (4.0 Å) and freshly distilled DCM (4.0 mL) at room temperature. The mixture was stirred overnight after which the iso(thio)cyanate (1.0 equiv.) was added. The progress of the reaction was monitored by TLC and MS, and after completion, the mixture was filtered through Celite and concentrated in vacuo. The residue was purified on silica gel, eluting with EtOAc/cHex (9:1 → 1:1). For all reactions in which an aromatic amine was employed, 6.6 equiv. of aldehyde were used.

Methyl 1-Butyl-5-(4-chlorophenyl)-4-phenyl-2-thioxoimidazolidine-4-carboxylate (4a5a): According to general procedure 2, the reaction between *n*-butylamine (146 mg; 2.00 mmol), 4-chlorobenzaldehyde (309 mg; 2.20 mmol) and methyl 2-(4-chlorophenyl)-2-isothiocyanatoacetate (**4a**; 242 mg; 1.00 mmol) afforded **4a5a** as a yellow foam (407 mg, 93 %, *dr* =47:53). ^1H NMR (250 MHz, $CDCl_3$): δ = 7.60 (d, *J* = 10.0 Hz, 2 H), 7.42 (d, *J* = 7.5 Hz, 2 H), 7.38 (d, *J* = 7.5 Hz, 2 H), 7.22 (d, *J* = 10.0 Hz, 2 H), 7.12–7.08 (m, 4 H), 7.03–6.99 (m, 2 H), 6.84–6.78 (m, 2 H), 6.50 (s, 1 H), 5.68 (s, 1 H), 4.9 (s, 1 H), 4.22–4.12 (m,1 H), 4.10–3.99 (m, 1 H), 3.82 (s, 3 H), 3.37 (s, 3 H), 2.79–2.69 (m, 1 H), 2.68–2.58 (m, 1 H), 1.57–1.42 (m, 2 H), 1.35–1.18 (m, 4 H), 1.12–0.97 (m, 2 H), 0.90 (t, *J* = 7.5 Hz, 3 H), 0.75 (t, *J* = 7.5 Hz, 3 H) ppm. The ^1H NMR spectrum matches that of the compound synthesized by another route reported by us earlier.[12a]

1′-Butyl-5′-(4-chlorophenyl)spiro[fluorene-9,4′-imidazolidine]-2′-thione (4c5a): According to general procedure 2, the reaction between *n*-butylamine (99 µL, 1.00 mmol), *p*-chlorobenzaldehyde (121 mg, 1.10 mmol) and 9-isothiocyanato-9*H*-fluorene (**4c**; 112 mg, 0.50 mmol) afforded **4c5a** as a white solid (153 mg, 73 %). M.p. 159.5–160.5 °C. ^1H NMR (500 MHz, $CDCl_3$): δ = 7.64 (d, *J* = 7.5 Hz, 1 H), 7.60 (d, *J* = 7.5 Hz, 1 H), 7.49 (d, *J* = 7.5 Hz, 1 H), 7.44 (t, *J* = 7.5 Hz, 1 H), 7.37 (t, *J* = 7.5 Hz, 1 H), 7.23 (t, *J* = 7.5 Hz, 1 H), 7.14 (d, *J* = 8.5 Hz, 2 H), 6.95 (t, *J* = 7.5 Hz, 1 H), 6.75 (d, *J* = 7.0 Hz, 2 H), 6.68 (d, *J* = 8 Hz, 1 H), 5.96 (s, 1 H), 5.10 (s, 1 H), 4.42 (ddd, *J* = 13.5, 10.0, 6.5 Hz, 1 H), 2.96 (ddd, *J* = 13.5, 10.0, 5.0 Hz, 1 H), 1.71–1.68 (m, 1 H), 1.58–1.52 (m, 1 H), 1.41–1.29 (m, 2 H), 0.92 (t, *J* = 7.0 Hz, 3 H) ppm. ^{13}C NMR (125 MHz, $CDCl_3$): δ = 185.1 (C), 147.6 (C), 141.4 (C), 140.2 (C), 139.3 (C), 134.6 (C), 132.8 (C), 130.0 (CH), 129.7 (CH), 129.0 (CH), 128.7 (2 CH), 127.5 (CH), 126.2 (CH), 125.3 (CH), 123.3 (CH), 120.4 (CH), 120.2 (CH), 120.1 (CH), 72.9 (C), 72.7 (CH), 45.44 (CH_2), 28.9 (CH_2), 20.3 (CH_2), 13.9 (CH_3) ppm. IR (neat): $\tilde{\nu}_{max}$ = 3138, 2926, 1489, 1458, 1448, 1281, 1190, 1144, 1090, 1011, 764, 733 cm^{-1}. HRMS (ESI): calcd. for $C_{25}H_{24}ClN_2S^+$ 419.1343; found 419.1361.

1′-Butyl-5′-(4-methoxyphenyl)spiro[fluorene-9,4′-imidazolidine]-2′-thione (4c5c): According to general procedure 2, the reaction between *n*-butylamine (73 mg, 1.00 mmol), *p*-methoxybenzaldehyde (151 mg, 1.10 mmol) and 9-isothiocyanato-9*H*-fluorene (**4c**; 112 mg, 0.50 mmol) afforded imidazolidine-2-thione **4c5c** as a yellow foam (166 mg, 80 %). ^1H NMR (500 MHz, $CDCl_3$): δ = 7.63 (d, *J* = 7.5 Hz, 1 H), 7.58 (d, *J* = 7.5 Hz, 1 H), 7.47 (d, *J* = 7.5 Hz, 1 H), 7.41 (t, *J* = 7.5 Hz, 1 H), 7.34 (t, *J* = 7.5 Hz, 1 H), 7.20 (t, *J* = 7.5 Hz, 1 H), 6.91 (t, *J* = 7.5 Hz, 1 H), 6.76–6.71 (m, 2 H), 6.67 (t, *J* = 8.5 Hz, 1 H), 6.01 (s, 1 H), 5.07 (s, 1 H), 4.43–4.36 (m, 1 H), 3.72 (s, 3 H), 2.99–2.94 (m, 1 H), 1.74–1.64 (m, 1 H), 1.60–1.49 (m, 1 H), 1.43–1.28 (m, 2 H), 0.92 (t, *J* = 7.0 Hz, 3 H) ppm. ^{13}C NMR (125 MHz): δ = 184.6 (C), 159.6 (C), 147.8 (C), 141.5 (C), 140.0 (C), 139.0 (C), 129.5 (CH), 129.2 (CH), 128.7 (CH), 128.4 (CH), 127.1 (CH), 126.2 (CH), 126.0 (C), 123.0 (CH), 120.0 (CH), 119.6 (CH), 113.6 (CH), 72.8 (C), 72.7 (CH), 55.1 (CH_3), 45.1 (CH_2), 28.9 (CH_2), 20.1 (CH_2), 13.7 (CH_3) ppm. IR: $\tilde{\nu}_{max}$ = 3067, 3009, 2957, 2930, 2837, 2735, 1682, 1597, 1578, 1510, 1448, 1425, 1302, 1248, 1215, 1192, 1177, 1159, 1109, 1026, 833,

766, 733 cm^{-1}. HRMS (ESI): calcd. for $C_{26}H_{27}N_2OS^+$ 415.1844; found 415.1809.

1′,5′-Dibutylspiro[fluorene-9,4′-imidazolidine]-2′-thione (4c5d): According to general procedure 2, the reaction between *n*-butylamine (99 μL, 1.00 mmol), valeraldehyde (117 μL, 1.10 mmol) and 9-isothiocyanato-9*H*-fluorene (**4c**; 112 mg, 0.50 mmol) afforded **4c5d** as a white solid (53 mg, 23 %). M.p. 125.1–125.6 °C. ^{1}H NMR (500 MHz, $CDCl_3$): δ = 7.64 (t, *J* = 8.0 Hz, 2 H), 7.55 (d, *J* = 7.5 Hz, 1 H), 7.47 (d, *J* = 7.5 Hz, 1 H), 7.43–7.40 (m, 2 H), 7.34 (td, *J* = 7.5, 0.5 Hz, 1 H), 7.28 (td, *J* = 7.0, 0.5 Hz, 1 H), 5.74 (s, 1 H), 4.25 (dd, *J* = 10.5, 4.0 Hz, 1 H), 4.04 (ddd, *J* = 14.5, 9.5, 6.5 Hz, 1 H), 3.50 (ddd, *J* = 12.5, 9.5, 7.0 Hz, 1 H), 1.69–1.61 (m, 2 H), 1.47–1.43 (m, 2 H), 1.34–1.28 (m, 1 H), 1.01 (t, *J* = 7.0 Hz, 3 H), 0.93–0.81 (m, 3 H), 0.65–0.57 (m, 1 H), 0.45 (t, *J* = 7.5 Hz, 3 H), 0.44–0.38 (m, 1 H) ppm. ^{13}C NMR (125 MHz, $CDCl_3$): δ = 183.9 (C), 145.7 (C), 143.3 (C), 140.5 (C), 140.1 (C), 130.0 (CH), 129.9 (CH), 128.4 (CH), 128.2 (CH), 125.6 (CH), 124.5 (CH), 120.5 (CH), 120.3 (CH), 72.2 (C), 68.2 (CH), 44.9 (CH_2), 29.3 (CH_2), 28.5 (CH_2), 26.8 (CH_2), 22.2 (CH_2), 20.4 (CH_2), 14.1 (CH_3), 13.4 (CH_3) ppm. IR (neat): $\tilde{\nu}_{max}$ = 3163, 2954, 2925, 2858, 1489, 1448, 1191, 732 cm^{-1}. HRMS (ESI): calcd. for $C_{23}H_{29}N_2S^+$ 365.2046; found 365.2028.

4-(1′-Butyl-2′-thioxospiro[fluorene-9,4′-imidazolidin]-5′-yl)-benzonitrile (4c5e): According to general procedure 2, the reaction between *n*-butylamine (99 μL, 1.00 mmol), *p*-cyanobenzaldehyde (144 mg, 1.10 mmol) and 9-isothiocyanato-9*H*-fluorene (**4c**; 112 mg, 0.50 mmol) afforded **4c5e** as a white solid [20 mg, 10 %; yield based on ^{1}H NMR relative to the doublet at δ = 7.97 ppm (4-cyanobenzaldehyde, 2 H)]. M.p. 161.3–162.6 °C. ^{1}H NMR (500 MHz, $CDCl_3$): δ = 7.64 (d, *J* = 7.5 Hz, 1 H), 7.59 (d, *J* = 7.5 Hz, 1 H), 7.48–7.43 (m, 4 H), 7.22 (t, *J* = 7.5 Hz, 2 H), 6.93–6.91 (m, 3 H), 6.63 (d, *J* = 8.0 Hz, 1 H), 6.07 (s, 1 H), 5.17 (s, 1 H), 4.44 (ddd, *J* = 14.0, 10.0, 6.5 Hz, 1 H), 2.94 (ddd, *J* = 14.0, 9.5, 5.0 Hz, 1 H), 1.71–1.67 (m, 1 H), 1.55–1.51 (m, 1 H), 1.41–1.31 (m, 2 H), 0.92 (t, *J* = 7.0 Hz, 3 H) ppm. ^{13}C NMR (125 MHz, $CDCl_3$): δ = 185.4 (C), 147.2 (C), 141.1 (C), 140.1 (C), 139.8 (C), 139.2 (C), 132.3 (2 CH), 130.2 (CH), 130.0 (CH), 130.0 (CH), 128.8 (CH), 128.3 (CH), 127.5 (CH), 125.9 (CH), 123.3 (CH), 120.5 (CH), 120.3 (CH), 118.4 (C), 112.6 (C), 72.8 (C), 72.8 (CH), 45.6 (CH_2), 29.8, 28.8 (CH_2), 20.2 (CH_2), 13.9 (CH_3) ppm. IR (neat): $\tilde{\nu}_{max}$ = 3151, 2230, 1448, 1281, 1188, 1143, 879, 731, 590, 551 cm^{-1}. HRMS (ESI): calcd. for $C_{26}H_{24}N_3S^+$ 410.1685; found 410.1680.

1′,5′-Bis(4-methoxyphenyl)spiro[fluorene-9,4′-imidazolidine]-2′-thione (4c5f): According to general procedure 2, the reaction between *p*-anisidine (123 mg, 1.0 mmol), 4-methoxybenzaldehyde (828 μL, 6.6 mmol) and 9-isothiocyanato-9*H*-fluorene (**4c**; 112 mg, 0.5 mmol) afforded imidazolidine-2-thione **4c5f** in trace amounts. HRMS (ESI): calcd. for $C_{29}H_{24}N_2NaO_2S$ 487.1451; found 487.1462.

5′-Butyl-1′-(4-methoxyphenyl)spiro[fluorene-9,4′-imidazolidine]-2′-thione (4c5g): According to general procedure 2, the reaction between *p*-anisidine (123 mg, 1.00 mmol), valeraldehyde (351 μL, 3.30 mmol) and 9-isothiocyanato-9*H*-fluorene (**4c**; 112 mg, 0.50 mmol) afforded **4c5g** as a yellow oil [41 mg, 20 %; yield based on ^{1}H NMR relative to the doublet at δ = 6.08 ppm (2 H)]. ^{1}H NMR (500 MHz, $CDCl_3$): δ = 4.60 (dd, *J* = 9.5, 4.5 Hz, 1 H) ppm. IR (neat): $\tilde{\nu}_{max}$ = 2926, 1508, 1448, 1437, 1244, 1028, 737 cm^{-1}. HRMS (ESI): calcd. for $C_{26}H_{27}N_2OS^+$ 415.1839; found 415.1825.

Methyl 1-Butyl-5-(4-methoxyphenyl)-4-phenyl-2-thioxoimidazolidine-4-carboxylate (4e5c): According to general procedure 2, the reaction between *n*-butylamine (99 μL, 1.00 mmol), *p*-methoxybenzaldehyde (144 mg, 1.10 mmol) and methyl (*S*)-2-isothiocyanato-2-phenylacetate (**4e**; 104 mg, 0.50 mmol) afforded **4e5c** as a yellow solid (diastereomer 1, 68 mg) and a yellow oil (diastereomer 2, 78 mg) (total yield 37 %, *dr* = 47:53).

Diastereomer 1: M.p. 128.8–130.7 °C. ^{1}H NMR (500 MHz, $CDCl_3$): δ = 7.10–7.08 (m, 3 H), 7.06–7.04 (m, 2 H), 6.83–6.69 (m, 2 H), 6.57 (d, *J* = 7.5 Hz, 2 H), 6.47 (s, 1 H), 5.67 (s, 1 H), 4.14 (ddd, *J* = 13.5, 8.0, 8.0 Hz, 1 H), 3.79 (s, 3 H), 3.66 (s, 3 H), 2.75 (ddd, *J* = 14.5, 7.5, 5.5 Hz, 1 H), 1.54–1.50 (m, 2 H), 1.32–1.23 (m, 2 H), 0.89 (t, *J* = 7.5 Hz, 3 H) ppm. ^{13}C NMR (125 MHz, $CDCl_3$): δ = 182.7 (C), 172.0 (C), 159.6 (C), 134.5 (C), 128.5 (*n* CH), 128.5 (*n* CH), 125.9 (*n* CH), 125.4 (C), 113.7 (*n* CH), 73.0 (C), 70.1 (CH), 55.3 (CH_3), 53.7 (CH_3), 45.0 (CH_2), 29.1 (CH_2), 19.9 (CH_2), 13.9 (CH_3) ppm. IR (neat): $\tilde{\nu}_{max}$ = 3175, 2959, 1730, 1608, 1508, 1448, 1231, 1205, 1038, 932, 827, 692 cm^{-1}. HRMS (ESI): calcd. for $C_{22}H_{27}N_2O_3S^+$ 399.1737; found 399.1729.

Diastereomer 2: ^{1}H NMR (500 MHz, $CDCl_3$): δ = 7.64 (d, *J* = 7.5 Hz, 2 H), 7.45–7.38 (m, 3 H), 7.21 (d, *J* = 8.5 Hz, 2 H), 6.90 (d, *J* = 8.5 Hz, 2 H), 6.76 (s, 1 H), 4.98 (s, 1 H), 4.05 (ddd, *J* = 14.0, 8.0, 8.0 Hz, 1 H), 3.82 (s, 3 H), 3.33 (s, 3 H), 2.67 (ddd, *J* = 13.5, 8.0, 6.0 Hz, 1 H), 1.34–1.25 (m, 2 H), 1.05–1.01 (m, 2 H), 0.73 (t, *J* = 7.0 Hz, 3 H) ppm. ^{13}C NMR (125 MHz, $CDCl_3$): δ = 181.6 (C), 168.6 (C), 160.3 (C), 140.1 (C), 129.1 (*n* CH), 129.0 (*n* CH), 127.0 (C), 125.5 (*n* CH), 114.3 (*n* CH), 74.7 (CH), 72.8 (C), 55.4 (CH_3), 52.8 (CH_3), 44.3 (CH_2), 29.3 (CH_2), 19.6 (CH_2), 13.7 (CH_3) ppm. IR (neat$\tilde{\nu}_{max}$ = 3190, 2955, 1742, 1610, 1512, 1445, 1246, 1177, 1030, 733, 696 cm^{-1}. HRMS (ESI): calcd. for $C_{22}H_{27}N_2O_3S^+$ 399.1737; found 399.1729.

Methyl 1,5-Dibutyl-4-phenyl-2-thioxoimidazolidine-4-carboxylate (4e5d): According to general procedure 2, the reaction between *n*-butylamine (99 μL, 1.00 mmol), valeraldehyde (117 μL, 1.10 mmol) and methyl 2-isothiocyanato-2-phenylacetate (**4e**; 104 mg, 0.50 mmol) afforded **4e5d** as a yellow oil (66 mg, 38 %) as a 1:1 mixture of diastereomers. ^{1}H NMR (500 MHz, $CDCl_3$): δ = 7.53–7.52 (m, 1 H + 1 H), 7.39–7.34 (m, 4 H + 4 H), 6.62 (s, 1 H), 6.38 (s, 1 H), 4.70–4.68 (m, 1 H), 4.20 (ddd, *J* = 14.5, 8.5, 7.0 Hz, 1 H), 4.12–4.07 (m, 1 H), 3.75 (s, 3 H), 3.74 (s, 3 H), 3.04 (ddd, *J* = 14.0, 8.5, 5.0 Hz, 1 H), 2.93 (ddd, *J* = 14.0, 8.0, 5.0 Hz, 1 H), 2.09–2.06 (m, 1 H), 1.82–1.77 (m, 1 H), 1.64–1.55 (m, 2 H), 1.01–0.77 (m, 7 H), 0.72 (t, *J* = 7.0 Hz, 3 H), 0.58 (t, *J* = 7.5 Hz, 3 H) ppm. ^{13}C NMR (125 MHz, $CDCl_3$): δ = 182.2 (C), 180.9 (C), 172.4 (C), 169.1 (C), 140.4 (C), 134.1 (C), 129.1 (*n* CH), 129.1 (*n* CH), 128.9 (*n* CH), 126.3 (*n* CH), 125.1 (*n* CH), 72.4 (C), 70.6 (CH), 70.3 (C), 65.0 (CH), 53.7 (CH_3), 53.1 (CH_3), 44.8 (CH_2), 44.0 (CH_2), 29.4 (CH_2), 29.2 (CH_2), 29.0 (CH_2), 28.1 (CH_2), 26.0 (CH_2), 25.7 (CH_2), 23.0 (CH_2), 22.5 (CH_2), 20.0 (CH_2), 19.5 (CH_2), 14.0 (CH_3), 14.0 (CH_3), 13.7 (CH_3), 13.6 (CH_3) ppm. IR (neat): $\tilde{\nu}_{max}$ = 2955, 2926, 2856, 1736, 1487, 1431, 1234, 1204, 731, 698 cm^{-1}. HRMS (ESI): calcd. for $C_{19}H_{29}N_2O_2S^+$ 349.1944; found 349.1950.

Methyl 1-Butyl-5-(4-cyanophenyl)-4-phenyl-2-thioxoimidazolidine-4-carboxylate (4e5e): According to general procedure 2, the reaction between *n*-butylamine (99 μL, 1.00 mmol), *p*-cyanobenzaldehyde (144 mg, 1.10 mmol) and methyl (*S*)-2-isothiocyanato-2-phenylacetate (**4e**; 104 mg, 0.50 mmol) afforded **4e5e** as a 2:1 mixture of diastereoisomers of which only the minor isomer was fully isolated as a red solid (45 mg, 23 %). M.p. 154.6–158.1 °C. ^{1}H NMR (500 MHz, $CDCl_3$): δ = 7.36 (d, *J* = 8.5 Hz, 2 H), 7.12–7.10 (m, 3 H), 7.03–7.02 (m, 4 H), 6.58 (s, 1 H), 5.77 (m, 1 H), 4.21 (ddd, *J* = 14.0, 8.0, 8.0 Hz, 1 H), 3.82 (s, 3 H), 2.72 (ddd, *J* = 14.0, 8.0, 6.0 Hz, 1 H), 1.54–1.50 (m, 2 H), 1.31–1.25 (m, 2 H), 0.90 (t, *J* = 7.5 Hz, 3 H) ppm. ^{13}C NMR (125 MHz, $CDCl_3$): δ = 183.3 (C), 171.4 (C), 139.3 (C), 133.6 (C), 132.1 (CH), 129.5 (CH), 128.8 (2 CH), 125.7 (2 CH), 118.3 (C), 117.9 (CH), 112.5 (C), 73.0 (C), 69.8 (CH), 54.0 (CH_3), 45.3 (CH_2), 29.1 (CH_2), 19.9 (CH_2), 13.9 (CH_3) ppm. IR (neat): $\tilde{\nu}_{max}$ = 3136, 2955, 2231, 1737, 1481, 1244, 1148, 1059, 842, 689, 550 cm^{-1}. HRMS (ESI): calcd. for $C_{22}H_{24}N_3O_2S^+$ 394.1584; found 394.1587.

Methyl 5-Butyl-1-(4-methoxyphenyl)-4-phenyl-2-thioxoimidazolidine-4-carboxylate (4e5g): According to general procedure 2, the reaction between *p*-anisidine (123 mg, 1.00 mmol), valeralde-

hyde (702 µL, 6.60 mmol) and methyl 2-isothiocyanato-2-phenylacetate (**4e**; 104 mg, 0.50 mmol) afforded **4e5g** in trace amounts. HRMS (ESI): calcd. for $C_{22}H_{27}N_2O_3S^+$ 399.1737; found 399.1727.

Acknowledgments

F. J. J. de Kanter and A. W. Ehlers are kindly acknowledged for maintaining the NMR facilities. The Ministerio de Ciencia e Innovacion (MICINN), the Fundacion Española para la Ciencia y la Tecnologıa (FECYT), the National Research School of Combination – Catalysis (NRSC-C), the Netherlands Organization for Scientific Research (NWO-CW, NWO-NCF, NWO-EW) and the Dutch Astrochemistry Network (DAN) supported by NWO are all acknowledged for funding.

Keywords: Multicomponent reactions · Computer chemistry · Synthesis design · Density functional calculations · Nitrogen heterocycles

[1] a) G. O. Jones, X. Li, A. E. Hayden, K. N. Houk, S. J. Danishefsky, *Org. Lett.* **2008**, *10*, 4093–4096; b) J. Mancebo-Aracil, C. Nájera, L. M. Castelló, J. M. Sansano, O. Larrañaga, A. de Cózar, F. P. Cossío, *Tetrahedron* **2015**, *71*, 9645–9661; c) L. P. Wolters, F. M. Bickelhaupt, *WIREs Comput. Mol. Sci.* **2015**, *5*, 324–343.

[2] a) R. C. Cioc, E. Ruijter, R. V. A. Orru, *Green Chem.* **2014**, *16*, 2958–2975; b) A. Dömling, W. Wang, K. Wang, *Chem. Rev.* **2012**, *112*, 3083–3135; c) J. Zhu, H. Bienaymé, *Multicomponent Reactions*, Wiley-VCH, Weinheim, **2005**; d) J. E. Biggs-Houck, A. Younai, J. T. Shaw, *Curr. Opin. Chem. Biol.* **2010**, *14*, 371–382.

[3] For recent examples, see: a) A. Milo, A. J. Neel, F. D. Toste, M. S. Sigman, *Science* **2015**, *347*, 737–743; b) Z. L. Niemeyer, A. Milo, D. P. Hickey, M. S. Sigman, *Nat. Chem.* **2016**, *8*, 610–617; c) R. P. Orenha, R. T. Santiago, R. L. A. Haiduke, S. E. Galembeck, *J. Comput. Chem.* **2017**, *38*, 883–981.

[4] I. W.-S. Lin, C.-N. Lok, K. Yan, C.-M. Che, *Chem. Commun.* **2013**, *49*, 3297–3299.

[5] P. Y. Lam, P. K. Jadhav, C. J. Eyermann, C. N. Hodge, Y. Ru, L. T. Bacheler, J. L. Meek, M. J. Otto, M. M. Rayner, Y. N. Wong, C.-H. Chang, P. Weber, D. A. Jackson, T. R. Sharpe, S. Erickson-Viitanen, *Science* **1994**, *263*, 380–384.

[6] a) M. K. Denk, A. Thadani, K. Hatano, A. J. Lough, *Angew. Chem. Int. Ed. Engl.* **1997**, *36*, 2607–2609; *Angew. Chem.* **1997**, *109*, 2719; b) N. Kuhn, T. Kratz, *Synthesis* **1993**, 561–562.

[7] a) R. S. Bon, B. van Vliet, N. E. Sprenkels, R. F. Schmitz, F. J. J. de Kanter, C. V. Stevens, M. Swart, F. M. Bickelhaupt, M. B. Groen, R. V. A. Orru, *J. Org. Chem.* **2005**, *70*, 3542–3553; b) N. Elders, R. F. Schmitz, F. J. J. de Kanter, E. Ruijter, M. B. Groen, R. V. A. Orru, *J. Org. Chem.* **2007**, *72*, 6135–6142; c) N. Elders, D. van der Born, L. J. D. Hendrickx, B. J. J. Timmer, A. Krause, E. Janssen, F. J. J. de Kanter, E. Ruijter, R. V. A. Orru, *Angew. Chem. Int. Ed.* **2009**, *48*, 5856–5859; *Angew. Chem.* **2009**, *121*, 5970.

[8] a) B. Ganem, *Acc. Chem. Res.* **2009**, *42*, 463–472; b) E. Ruijter, R. Scheffelaar, R. V. A. Orru, *Angew. Chem. Int. Ed.* **2011**, *50*, 6234–6246; *Angew. Chem.* **2011**, *123*, 6358.

[9] W. Y. Han, J. Q. Zhao, J. Zuo, X. Y. Xu, X. M. Zhang, W. C. Yuan, *Adv. Synth. Catal.* **2015**, *357*, 3007–3031.

[10] a) R. A. Volkmann, J. T. Davis, C. N. Meltz, *J. Am. Chem. Soc.* **1983**, *105*, 5946–5948; b) C. N. Meltz, R. A. Volkmann, *Tetrahedron Lett.* **1983**, *24*, 4503–4506.

[11] a) H.-W. Zhao, B. Li, T. Tian, X.-Q. Song, H.-L. Pang, X.-Q. Chen, Z. Yang, W. Meng, *RSC Adv.* **2016**, *6*, 27690–27695; b) Y.-Y. Han, W.-B. Chen, W.-Y. Han, Z.-J. Wu, X.-M. Zhang, W.-C. Yuan, *Org. Lett.* **2012**, *14*, 490–493; c) H. Cai, Y. Zhou, D. Zhang, J. Xu, H. Liu, *Chem. Commun.* **2014**, *50*, 14771–14774.

[12] a) R. S. Bon, N. E. Sprenkels, M. M. Koningstein, R. F. Schmitz, F. J. J. de Kanter, A. Domling, M. B. Groen, R. V. A. Orru, *Org. Biomol. Chem.* **2008**, *6*, 130–137; b) M. Mooijman, R. S. Bon, N. E. Sprenkels, H. N. van Oosterhout, F. J. J. de Kanter, M. B. Groen, E. Ruijter, R. V. A. Orru, *Synlett* **2012**, *23*, 80–84.

[13] J. S. Nowick, N. A. Powell, T. M. Nguyen, G. Noronha, *J. Org. Chem.* **1992**, *57*, 7364–7366.

[14] Instead of a homogeneous base, Na_2CO_3 was employed.

[15] For the optimization table, see the Supporting Information.

[16] R. S. Bon, C. G. Hong, M. J. Bouma, R. F. Schmitz, F. J. J. de Kanter, M. Lutz, A. L. Spek, R. V. A. Orru, *Org. Lett.* **2003**, *5*, 3759–3762.

[17] G. V. Janssen, P. Slobbe, M. Mooijman, A. Kruithof, A. W. Ehlers, C. F. Guerra, F. M. Bickelhaupt, J. C. Slootweg, E. Ruijter, K. Lammertsma, R. V. A. Orru, *J. Org. Chem.* **2014**, *79*, 5219–5226.

[18] a) E. J. Baerends, T. Ziegler, J. Autschbach, D. Bashford, A. Bérces, F. M. Bickelhaupt, C. Bo, P. M. Boerrigter, L. Cavallo, D. P. Chong, L. Deng, R. M. Dickson, D. E. Ellis, M. van Faassen, L. Fan, T. H. Fischer, C. Fonseca Guerra, M. Franchini, A. Ghysels, A. Giammona, S. J. A. van Gisbergen, A. W. Götz, J. A. Groeneveld, O. V. Gritsenko, M. Grüning, S. Gusarov, F. E. Harris, P. van den Hoek, C. R. Jacob, H. Jacobsen, L. Jensen, J. W. Kaminski, G. van Kessel, F. Kootstra, A. Kovalenko, M. V. Krykunov, E. van Lenthe, D. A. McCormack, A. Michalak, M. Mitoraj, S. M. Morton, J. Neugebauer, V. P. Nicu, L. Noodleman, V. P. Osinga, S. Patchkovskii, M. Pavanello, P. H. T. Philipsen, D. Post, C. C. Pye, W. Ravenek, J. I. Rodríguez, P. Ros, P. R. T. Schipper, H. van Schoot, G. Schreckenbach, J. S. Seldenthuis, M. Seth, J. G. Snijders, M. Solà, M. Swart, D. Swerhone, G. te Velde, P. Vernooijs, L. Versluis, L. Visscher, O. Visser, F. Wang, T. A. Wesolowski, E. M. van Wezenbeek, G. Wiesenekker, S. K. Wolff, T. K. Woo, A. L. Yakovlev, *ADF2014*, SCM, Theoretical Chemistry, Vrije Universiteit, Amsterdam, http://www.scm.com; b) C. Fonseca Guerra, J. G. Snijders, G. te Velde, E. J. Baerends, *Theor. Chem. Acc.* **1998**, *99*, 391–403; c) G. te Velde, F. M. Bickelhaupt, E. J. Baerends, C. Fonseca Guerra, S. J. A. van Gisbergen, J. G. Snijders, T. Ziegler, *J. Comput. Chem.* **2001**, *22*, 931–967.

[19] M. Swart, F. M. Bickelhaupt, *J. Comput. Chem.* **2008**, *29*, 724–734.

[20] a) A. Klamt, G. Schuurmann, *J. Chem. Soc. Perkin Trans. 2* **1993**, 799–805; b) C. C. Pye, T. Ziegler, *Theor. Chem. Acc.* **1999**, *101*, 396–408.

[21] Attempts to quantify this proton shift by means of a TS analysis were unsuccessful.

[22] The barrier of this hypothetical concerted reaction was calculated and gave a relative barrier of 39.7 kcal/mol, see the overview in the Supporting Information for more information.

[23] a) P. W. Atkins, *Physical Chemistry*, 8th ed., Freeman, New York, **2006**; b) M. Swart, E. Rösler, F. M. Bickelhaupt, *Eur. J. Inorg. Chem.* **2007**, 3646–3654.

[24] For all anilines, 6 equiv. of aldehyde were employed to exclude urea formation caused by incomplete imine formation.

[25] The color scheme is derived from the reactivity/ΔPA relation in the two above-mentioned sets of experiments, and is meant to highlight the observations discussed hereafter.

[26] M. Swart, F. M. Bickelhaupt, *Computer Code QUILD* (QUantum regions Interconnected by Local Description), Vrije Universiteit, Amsterdam, **2006**.

[27] E. van Lenthe, E. J. Baerends, *J. Comput. Chem.* **2003**, *24*, 1142–1156.

[28] E. van Lenthe, E. J. Baerends, J. G. Snijders, *J. Chem. Phys.* **1993**, *99*, 4597–4610.

[29] J. C. Slater, *Phys. Rev.* **1951**, *81*, 385–390.

[30] S. H. Vosko, L. Wilk, M. Nusair, *Can. J. Phys.* **1980**, *58*, 1200–1211.

[31] N. C. Handy, A. J. Cohen, *Mol. Phys.* **2001**, *99*, 403–412.

[32] a) B. G. Johnson, P. M. W. Gill, J. A. Pople, *J. Chem. Phys.* **1993**, *98*, 5612–5626; b) C. Lee, W. Yang, R. G. Parr, *Phys. Rev. B* **1988**, *37*, 785–789; c) T. V. Russo, R. L. Martin, P. J. Hay, *J. Chem. Phys.* **1994**, *101*, 7729–7737.

[33] N. L. Allinger, X. Zhou, J. Bergsma, *J. Mol. Struct.* **1994**, *312*, 69–83.

[34] a) J. L. Pascual-Ahuir, E. Silla, *J. Comput. Chem.* **1990**, *11*, 1047–1060; b) J. L. Pascual-Ahuir, E. Silla, I. Tuñon, *J. Comput. Chem.* **1994**, *15*, 1127–1138; c) E. Silla, I. Tuñón, J. L. Pascual-Ahuir, *J. Comput. Chem.* **1991**, *12*, 1077–1088.

Received: July 4, 2017